ARTICLE

Elastic Behavior of Methyltrimethoxysilane Based Aerogels Reinforced with Tri-Isocyanate

Baochau N. Nguyen,*,† Mary Ann B. Meador,*,‡ Alexandra Medoro,§ Victoria Arendt,§ Jason Randall,|| Linda McCorkle,† and Brian Shonkwiler⊥

Ohio Aerospace Institute, 22800 Cedar Point Road, Brookpark, Ohio 44142, and NASA Glenn Research Center, 21000 Brookpark Road, Cleveland Ohio 44135

ABSTRACT The elastic properties and/or flexibility of polymer reinforced silica aerogels having methyltrimethoxysilane (MTMS) and bis(trimethoxysilylpropyl)amine (BTMSPA) making up the silica structure are examined. The dipropylamine spacer from BTMSPA is used both to provide a flexible linking group in the silica structure, and as a reactive site via its secondary amine for reaction with a tri-isocyanate, Desmodur N3300A. The tri-isocyanate provides an extended degree of branching or reinforcement, resulting in increased compressive strength of the aerogel monoliths while the overall flexibility arising from the underlying silica structure is maintained. The compressive moduli of the reinforced aerogel monoliths in this study range from 0.001 to 158 MPa. Interestingly, formulations across this entire range of modulus recover nearly all of their length after two compressions to 25% strain. Differences in pore structure of the aerogels due to processing conditions and solvent are also discussed.

KEYWORDS: aerogels • triisocyanate • cross-linking • mesoporous materials • hybrid materials • elastic recovery

INTRODUCTION

Silica aerogels with their low density and thermal conductivity are potential candidates for various thermal, optical, and acoustic applications for aerospace, including multipurpose structures for vehicles, space suits and habitats (1). However, the use of aerogel monoliths has been restricted because of their inherent fragility, hygroscopic nature, and poor mechanical properties. It has been demonstrated that a conformal coating of polymer over the skeletal nanostructure of the silica gel can be formed by reacting di-isocyanate with silanol groups on the surface (2). This improves the strength by as much as 2 orders of magnitude while only doubling the density over those of native or nonreinforced aerogels. In addition, the mesoporosity of these polymer reinforced aerogels and hence their superior insulation properties, among other things, is maintained. Incorporating a functional group such as amine, vinyl, or free-radical initiator into a silica-based aerogel improves the reactivity toward isocyanates (3, 4) and expands the types of organic monomers that can be used as reinforcement to include epoxides (5), cyanoacrylates (6), or styrene (7).

Although polymer reinforced aerogels exhibit a great improvement in strength over native silica aerogels, for many applications it is desirable to have a more flexible or elastic material. For example, insulation for extravehicular activity (EVA) suits should also be durable and flexible to accommodate as much freedom of movement for the astronaut as possible (8). A flexible form of polymer reinforced aerogel would also be desirable for wrapping around structures that need to be insulated, such as cryotanks or cryogenic transfer lines (9). Yet another use for flexible durable aerogels could be as part of an inflatable decelerator used to slow spacecraft for planetary entry, descent and landing (EDL) (10). EDL systems used to successfully land six robotic missions on Mars from 1976 to 2008 employed a hard aeroshell heat shield and parachutes of 12−16 m in diameter. Future robotic and manned missions are much heavier and will require more drag for landing. Hence, new designs with much larger diameters (30−60 m) will be required (11). Inflatable decelerators would stow in a small space and deploy into a large area lightweight heat shield to survive reentry (12). Minimizing weight and thickness of the system as well as providing suitable insulation are important considerations.

Though some measure of flexibility is obtained in the polymer reinforced aerogels through a decrease in density (4), it has been shown that more flexibility is obtained in nonreinforced aerogels by altering the silica backbone in some significant way. For example, Kramer et al. (13) demonstrated that including up to 20% (w/w) poly(dimethylsiloxane) in tetraethylorthosilicate (TEOS)-based aerogels resulted in rubbery behavior with up to 30% recoverable compressive strain. More recently, Rao et al. (14) have shown that utilizing methyltrimethoxysilane (MTMS) as the silica precursor and a two-step synthesis imparts extraordinary flexibility to the aerogels. The MTMS-derived aerogels are more flexible largely because of the resulting lower cross-link density of the silica (three alkoxy groups that can react

* To whom correspondence should be addressed. E-mail: Baochau.n.nguyen@nasa.gov (B.N.N.); maryann.meador@nasa.gov (M.A.B.M.).
Received for review January 29, 2010 and accepted April 13, 2010
† Ohio Aerospace Institute.
‡ NASA Glenn Research Center.
§ NASA LERCIP Summer Interns.
|| University of Akron, NASA Graduate Fellow.
⊥ Present address: Clark Atlanta University, Atlanta, GA 30314.
DOI: 10.1021/am100081a

Published on Web 04/28/2010

versus four in the more rigid tetra-alkoxysilane derived aerogels). Kanamori et al. (15), using a surfactant to control the pore size and a slightly different process, showed that MTMS-derived gels can be made which demonstrate reversible deformation on compression. In fact, some formulations were able to be dried ambiently, which exerts similar forces on the gels. Initially, the gels shrink about 65% but spring back to nearly their original size, resulting in almost identical density and pore structure as those dried supercritically.

Though the MTMS derived aerogels are very flexible and elastic, it does not take much force to compress them. For example, Rao (14) reports a Young's modulus of only 0.03 to 0.06 MPa for the flexible MTMS derived aerogels ranging in density from 0.04 to 0.1 g/cm^3. Kanamori (15) does not report Young's modulus, but stress−strain curves indicate that stresses of less than 1 MPa are sufficient to compress samples with bulk densities around 0.2 g/cm^3 to 25% strain. Other highly porous materials show similar elastic behavior after compression depending on density and backbone structure, including epoxy reinforced clay cryogels (16), starch-polystyrene foams (17), and cross-linked (18) or carbon-nanotube-reinforced (19) ethylene-vinyl acetate foams.

We recently demonstrated improved compressive strength combined with elastic recovery after compression for silica aerogels reinforced with styrene (20), epoxy (21), or di-isocyanate (22) by replacing a large fraction of TMOS or TEOS with bis(trimethoxysilyl)hexane (BTMSH). The hexyl group from BTMSH provides a flexible link in the underlying silica giving similar elastic properties as seen in MTMS-derived aerogels. Polymer reinforcement is provided as previously described by incorporating reactive groups in the silica backbone and reacting with monomer. In this way, polymer reinforced aerogels were made with compressive modulus as high as 10 MPa (100 times that of the MTMS gels), which still recovered almost completely from compression to 25% strain.

In this study, we wish to examine the effect of incorporating organic linking groups into the underlying silica structure and use of polymer reinforcement on MTMS-derived aerogels to preserve their unique spring back behavior while increasing the compressive strength. To this end, silica gels are prepared using MTMS and bis(trimethoxysilylpropyl)amine (BTMSPA) precursors in a one-step synthesis as shown in Scheme 1, using acetonitrile or acetone as the solvent. The secondary amine from the BTMSPA serves as the base to catalyze condensation of the silanes. It also provides a site for reaction with tri-isocyanate to form a polyurea conformal coating on the silica structure. A statistical experimental design is employed to examine the effect of total concentration of silicon in the gels derived from both BTMSPA and MTMS (noting that BTMSPA contributes two moles of silicon for every mole of silane), mol % of Si derived from BTMSPA, solvent used for the entire process of making the aerogels (acetone or acetonitrile), water/total silicon mol ratio (r), and the number of washes (to remove excess water and methanol byproduct from the hydrogels) before reacting with a tri-isocyanate on the mechanical and physical properties of the aerogels. Properties of the polymer reinforced aerogels are also compared to their nonreinforced counterparts.

EXPERIMENTAL SECTION

General. Methyltrimethoxysilane (MTMS) and bis(trimethoxysilylpropyl)amine (BTMSPA) were purchased from Gelest, Inc. Acetonitrile and acetone were obtained from Aldrich Chemical Co.. Liquid carbon dioxide was purchased from Air Gas Great Lake. Desmodur N3300A was provided by Bayer Corporation. All reagents were used without further purification.

Preparation of Silica Monoliths. Variables examined in aerogel preparation are the concentration of total silicon (derived from MTMS and BTMSPA combined) in the total solution (M), mole fraction of silicon derived from BTMSPA (mol %), solvent used for the entire fabrication process (acetonitrile or acetone), water/total silicon ratio (r), and the number of washes before the polymerization reaction with N3300A, or cross-linking reaction, as shown in Table 1. The silica gels were prepared using a one-step synthesis with BTMSPA acting as the base catalyst as well as a site for cross-linking with tri-isocyanate.

In a typical example, run 7 from Table 1 was made using 1.65 mol/L of total silane, with 20 mol % silicon from MTMS and 80 mol % silicon from BTMSPA (noting that BTMSPA contributes two moles of silicon for every mole of silane). A solution of 4.70 mL (33 mmol) of MTMS and 21.70 mL (66 mmol) of BTMSPA in 58.75 mL of acetonitrile was cooled to below 0 °C using a dry ice acetone bath. An amount of 14.85 mL (825 mmol) of H_2O was then added to the silane solution ($r = 5$), followed by thorough mixing before being poured into 20 mL plastic syringe molds. Gelation occurred within 15 min. The wet gels were aged for 24 h before being extracted into fresh acetonitrile and allowed to rest for another 24 h. The gels were then soaked in a 30% (w/w) solution of N3300A in acetonitrile for 24 h, followed by solvent exchange to fresh acetonitrile before being heated to 70 °C for 6 h. The polymer reinforced gels were washed in fresh acetonitrile four times at 24 h intervals before being dried using supercritical carbon dioxide (CO_2) extraction.

The corresponding nonreinforced aerogels listed in Table 2 were prepared the same way, except that soaking in tri-isocyanate and heat treatment steps were eliminated. In addition, the same procedure was used when acetonitrile was replaced with acetone as the fabrication solvent.

Instrumental. The skeletal density (ρ_s) was measured using an Accupyc 1340 helium pycnometer. Nitrogen sorption measurements using Brunauer−Emmett−Teller (BET) method were performed on a Micromeritics ASAP2020 chemisorption system. All samples were outgassed at 80 °C for 12 h under a vacuum before analysis. Samples for microscopy were coated with gold/palladium and viewed using a Hitachi S-4700-11 field emission scanning electron microscope. Supercritical CO_2 fluid extraction was performed using an Applied Separations 1-Speed SFE-2 manual system. Mechanical tests were done on an Instron 4505 eletromechanical machine using Testworks 4 software and a 10000 Newton load cell at 0.25 in./min. Solid ^{13}C and ^{29}Si NMR spectra were obtained on a Bruker Avance-300 spectrometer with a 4-mm solids probe using cross-polarization and magic angle spinning at 11 kHz. The ^{13}C NMR spectra were externally referenced to the carbonyl of glycine, which appears at 176.01 ppm, and the ^{29}Si NMR spectra were externally referenced to the Si of 3-trimethoxysilylpropionic acid, which is at 0 ppm.

Characterization. The bulk density (ρ_b) was determined by measuring the weight and volume of the sample. Dimensional change, or shrinkage (%), is taken as the difference between the diameters of the aerogel monolith and of the 20 mL syringe mold (nominally 20 mm). The skeletal density from helium

Scheme 1. Proposed Molecular Structure of Aerogels from MTMS and BTMSPA and Reinforced with Tri-isocyanate Desmodur N3300

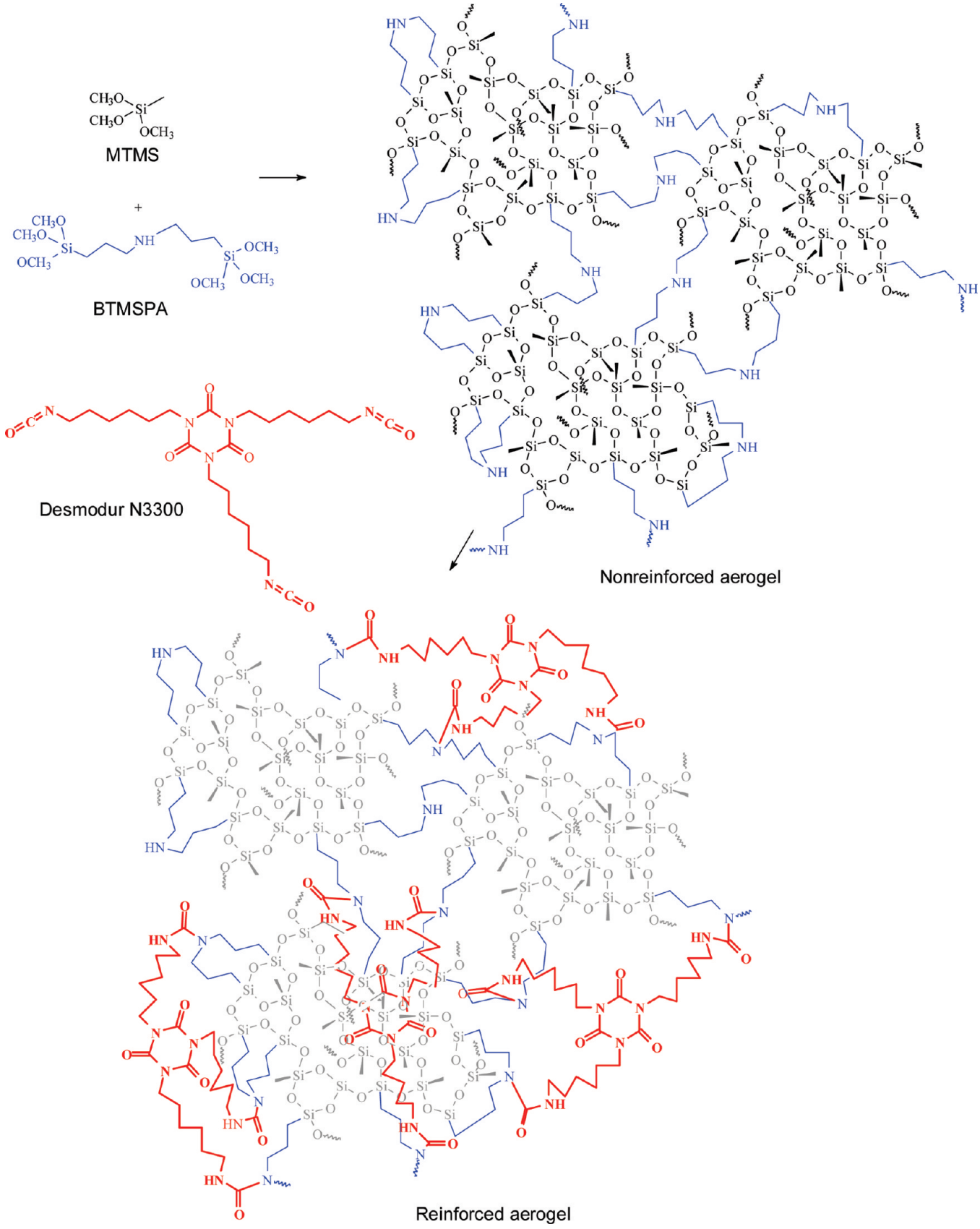

pycnometry (ρ_s) and the bulk density were used to calculate the porosity (%) of the aerogels using eq 1.

Compression tests were carried out on the aerogel monoliths in two steps. First, the aerogels were compressed to 25% strain.

$$\text{porosity } \% = \frac{1/\rho_b - 1/\rho_s}{1/\rho_b} \times 100 \qquad (1)$$

The test was stopped, the crosshead was instantly moved back to zero, and the procedure was repeated once more and released. The specimen was then left to sit for 30 min at room temperature. At that time, the final thickness was measured and the unrecovered strain (%) was determined as the amount of strain still present in the sample relative to the sample's initial length. The modulus was taken as the initial slope from the stress−strain curve of the first compression.

Statistical Analysis. Experimental design and analysis was conducted using Design Expert 7.1.3 available from Stat-Ease, Inc. Using a d-optimal design to minimize the number of experiments, a total of 40 distinct batches of the aerogel monoliths, including 5 repeats of one formulation (2, 12, 14, 15, and 18) were prepared by varying the total silicon concentration (0.75−1.65 mol/L), the fraction of silicon derived from BTMPSA (40 − 80 Si mol %), the water/silicon ratio ($r = 2 - 5$), the solvent (acetone or acetonitrile), and the number of washes (1−3) before the cross-linking reaction. Silicon concentration and silicon mole percent were used instead of silane concentration because every mole of BTMSPA contributes 2 mol of silicon, whereas 1 mol of MTMS contributes only 1 mol of silicon. Preparation conditions and measured properties of all of the polymer reinforced aerogels are listed in Table 1, whereas the nonreinforced (native) aerogels are listed in Table 2. The run

Table 1. Preparation Conditions and Measured Properties for Polymer Reinforced Aerogels

run	total Si (M)	MTMS (mol %)	BTMSPA (mol %)	water: silane	no. of washes	solvent	NCO: NH ratio	bulk density (g/cm^3)	porosity (%)	shrinkage (%)	BET surface area (m^2/g)	modulus (MPa)	max. stress at break (MPa)	toughness (kJ/m^3)	unrecovered strain (%)
1	0.75	60	40	2.0	1	acetonitrile	0.03	0.058	95.9	4.0	[a]	0.00	2.76×10^{-3}	0.4	1.6
2	1.20	40	60	3.5	2	acetonitrile	0.71	0.163	87.9	2.0	230.5	2.60	3.8	582	1.0
3	1.20	40	60	3.5	3	acetonitrile	0.71	0.160	88.5	2.0	237.6	2.69	4.1	631	1.1
4	1.65	20	80	5.0	3	acetonitrile	1.02	0.369	72.1	10.2	260.0	72.36	36.7	6488	2.1
5	0.75	20	80	5.0	3	acetonitrile	0.58	0.101	92.6	3.1	139.1	0.60	0.3	47	0.7
6	1.65	60	40	2.0	1	acetonitrile	0.72	0.187	85.8	1.2	292.3	2.94	4.3	662	3.2
7	1.65	20	80	5.0	1	acetonitrile	1.22	0.385	70.6	9.6	233.5	84.25	39.7	6944	3.0
8	1.20	40	60	5.0	2	acetonitrile	0.82	0.167	87.8	2.1	204.9	3.51	3.4	524	1.1
9	1.20	40	60	3.5	1	acetonitrile	0.94	0.163	90.2	2.1	203.9	3.12	2.6	437	0.7
10	1.20	40	60	2.0	2	acetonitrile	0.95	0.157	89.6	1.7	234.1	2.26	3.7	556	0.5
11	0.75	40	60	3.5	2	acetonitrile	0.05	0.072	95.4	2.0	18.1	0.02	0.0	5.1	1.1
12	1.20	40	60	3.5	2	acetonitrile	0.94	0.164	87.8	1.6	233.6	2.48	3.1	477	1.8
13	1.20	20	80	3.5	2	acetonitrile	1.01	0.216	84.2	4.9	248.1	10.55	12.3	1893	1.1
14	1.20	40	60	3.5	2	acetonitrile	0.77	0.157	88.5	1.8	231.6	2.74	2.9	448	1.3
15	1.20	40	60	3.5	2	acetonitrile	0.88	0.159	88.1	1.5	224.6	2.68	3.4	2085	0.7
16	0.75	20	80	2.0	1	acetonitrile	0.39	0.102	92.7	2.4	93.2	0.32	0.9	115	0.7
17	1.20	40	60	3.5	2	acetonitrile	0.69	0.160	88.5	2.2	229.1	2.38	2.8	383	0.7
18	1.20	40	60	3.5	2	acetonitrile	0.89	0.219	83.6	1.6	217.9	2.77	4.6	687	1.3
19	0.75	60	40	5.0	3	acetonitrile	0.01	0.053	96.9	2.8	[a]	0.01	9.7×10^{-3}	2.2	0.0
20	1.65	20	80	2.0	1	acetonitrile	1.03	0.356	72.9	8.9	266.1	49.98	41.9	6988	2.2
21	0.75	60	40	5.0	1	acetonitrile	0.01	0.049	97.0	1.9	7.4	0.01	1.0×10^{-3}	1.9	0.0
22	0.75	20	80	5.0	1	acetonitrile	0.50	0.105	92.6	2.3	126.2	0.50	0.4	71	0.6
23	1.65	60	40	5.0	3	acetonitrile	0.74	0.185	86.3	1.3	275.6	2.65	2.8	426	2.6
24	0.75	20	80	2.0	3	acetonitrile	0.46	0.100	92.5	1.8	102.9	0.31	1.0	105	2.0
25	1.20	60	40	3.5	2	acetonitrile	0.45	0.111	92.2	0.4	158.7	0.29	0.5	64	1.1
26	1.65	60	40	5.0	1	acetonitrile	1.02	0.185	86.7	1.2	246.8	2.48	3.2	488	3.5
27	1.65	20	80	2.0	3	acetonitrile	1.04	0.353	73.2	8.3	288.7	51.91	44.8	6405	2.1
28	1.65	60	40	2.0	3	acetonitrile	0.87	0.189	85.8	0.9	301.5	3.11	4.6	692	1.9
29	0.75	60	40	2.0	3	acetonitrile	0.17	0.056	96.4	3.8	[a]	0.00	4.8×10^{-3}	0.8	3.8
30	1.65	40	60	3.5	2	acetonitrile	1.05	0.275	79.1	4.8	242.2	17.65	23.2	3641	1.2
31	0.75	60	40	2.0	1	acetone	0.44	0.066	95.5	5.3	76.9	0.01	0.06	15	0.79
32	1.65	20	80	5.0	1	acetone	1.60	0.482	69.2	11.7	215.1	157.59	71.00	13082	0.56
33	0.75	40	60	3.5	2	acetone	0.75	0.109	93.0	4.7	256.8	0.22	1.65	218	0.44
34	1.20	40	60	3.5	2	acetone	1.13	0.184	87.2	4.6	283.7	3.60	8.54	1117	0.36
35	1.20	40	60	3.5	2	acetone	1.13	0.189	86.8	5.6	297.0	3.44	6.86	1091	0.79
36	0.75	20	80	2.0	1	acetone	1.17	0.138	90.2	5.4	275.8	1.00	1.01	351	0.33
37	0.75	60	40	5.0	1	acetone	0.26	0.066	96.0	4.0	119.6	0.02	0.07	10	1.20
38	0.75	20	80	2.0	3	acetone	0.99	0.130	90.8	5.2	253.3	0.76	3.04	363	0.74
39	1.65	60	40	5.0	1	acetone	2.14	0.327	75.6	6.4	210.7	29.24	20.03	347	0.92
40	0.75	60	40	2.0	3	acetone	0.62	0.073	95.8	5.2	147.3	0.03	0.2	36	0.36

[a] Samples collapsed under vacuum. No data were collected.

Table 2. Preparation Conditions and Measured Properties for Nonreinforced Aerogels

run	total Si (M)	MTMS (mol %)	BTMSPA (mol %)	water: silane	solvent	bulk density (g/cm^3)	porosity (%)	shrinkage (%)	BET surface area (m^2/g)	modulus (MPa)	max. stress at break (MPa)	toughness (kJ/m^3)	unrecovered strain (%)
1	0.75	60	40	2.0	acetonitrile	0.055	96.3	5.1	[a]	[a]	[a]	[a]	[a]
2	1.20	40	60	3.5	acetonitrile	0.126	90.9	4.0	[b]	1.94	0.93	153	0.5
3	1.20	40	60	3.5	acetonitrile	0.124	91.9	3.2	394.9	1.93	0.75	115	1.1
4	1.65	20	80	5.0	acetonitrile	0.242	82.0	11.7	531.2	48.78	5.61	775	NA
5	0.75	20	80	5.0	acetonitrile	0.085	93.8	4.0	215.2	0.48	0.25	39	2.3
6	1.65	60	40	2.0	acetonitrile	0.147	89.0	3.0	[b]	2.87	0.46	50	NA
7	1.65	20	80	5.0	acetonitrile	0.234	82.6	10.1	521.0	38.05	5.39	745	0.9
8	1.20	40	60	5.0	acetonitrile	0.124	90.8	2.2	521.0	1.78	0.82	132	0.08
9	1.20	40	60	3.5	acetonitrile	0.124	90.7	4.0	531.2	1.44	0.96	160	0.44
10	1.20	40	60	2.0	acetonitrile	0.131	90.2	5.1	385.1	2.13	0.95	152	0.2
11	0.75	40	60	3.5	acetonitrile	0.067	95.1	0.6	215.4	[a]	[a]	[a]	[a]
12	1.20	40	60	3.5	acetonitrile	0.125	90.7	3.2	387.7	2.11	0.35	40	NA
13	1.20	20	80	3.5	acetonitrile	0.153	88.0	6.1	477.3	7.18	2.44	422	0.8
14	1.20	40	60	3.5	acetonitrile	0.127	90.6	4.3	371.1	2.11	0.54	76	1.2
15	1.20	40	60	3.5	acetonitrile	0.128	90.6	3. 7	393.8	2.34	0.87	148	1.5
16	0.75	20	80	2.0	acetonitrile	0.087	94.0	5.3	134.7	0.11	0.13	21	0.85
17	1.20	40	60	3.5	acetonitrile	0.124	90.7	3.5	[b]	2.13	1.06	175	1.1
18	1.20	40	60	3.5	acetonitrile	0.130	69.7	4.4	392.6	2.21	0.90	144	0.2
19	0.75	60	40	5.0	acetonitrile	0.052	96.7	5.3	[a]	[a]	[a]	[a]	[a]
20	1.65	20	80	2.0	acetonitrile	0.256	81.0	13.3	499.8	45.66	2.33	322	NA
21	0.75	60	40	5.0	acetonitrile	0.054	96.4	4.5	[a]	[a]	[a]	[a]	[a]
22	0.75	20	80	5.0	acetonitrile	0.086	94.1	3.9	[b]	0.45	0.26	43	1.0
23	1.65	60	40	5.0	acetonitrile	0.159	88.5	3.3	[b]	1.92	1.13	173	0.52
24	0.75	20	80	2.0	acetonitrile	0.093	93.1	5.1	122.2	0.31	0.48	73	0.1
25	1.20	60	40	3.5	acetonitrile	0.104	92.1	2.3	[b]	0.31	0.19	28	0.4
26	1.65	60	40	5.0	acetonitrile	0.155	88.4	3.8	412.5	2.14	0.99	148	0.6
27	1.65	20	80	2.0	acetonitrile	0.265	80.4	13.2	[b]	39.38	7.08	1171	1.4
28	1.65	60	40	2.0	acetonitrile	0.168	74.5	4.5	402.7	2.67	4.48	725	0.6
29	0.75	60	40	2.0	acetonitrile	0.055	96.3	5.1	[a]	[a]	[a]	[a]	[a]
30	1.65	40	60	3.5	acetonitrile	0.214	84.6	7.9	[b]	12.08	6.53	1126	1.3
31	0.75	60	40	2.0	acetone	0.061	96.45	9.2	179.9	0.02	0.10	9	0.00
32	1.65	20	80	5.0	acetone	0.287	80.34	14.7	589.6	41.23	12.72	2270	4.08
33	0.75	40	60	3.5	acetone	0.093	94.15	7.7	374.8	0.20	0.22	36	0.00
34	1.20	40	60	3.5	acetone	0.133	91.37	6.8	507.7	1.89	0.51	106	2.27
35	1.20	40	60	3.5	acetone	0.145	90.44	9.0	523.6	2.19	1.58	161	3.30
36	0.75	20	80	2.0	acetone	0.113	92.13	11.0	390.2	0.51	0.9	144	2.99
37	0.75	60	40	5.0	acetone	0.060	96.63	7.9	145.8	[a]	[a]	[a]	[a]
38	0.75	20	80	2.0	acetone	0.107	93.19	10.6	386.3	0.46	0.86	133	6.48
39	1.65	60	40	5.0	acetone	0.182	88.10	7.5	563.0	3.84	2.08	344	1.65
40	0.75	60	40	2.0	acetone	0.060	96.75	7.3	289.6	[a]	[a]	[a]	[a]

[a] Aerogels were not tested because of their softness and/or fragility. [b] No samples available for testing.

number represents a particular formulation made at once in a single batch. The order of preparation of individual formulations is random to reduce the correlation of systematic errors with any variable.

Data from Tables 1 and 2 were modeled using multiple linear least-squares regression analysis, considering a model including all first-order effects of the four variables, as well as all two-way interactions. All of the variables were orthogonalized (transformed to a -1 to $+1$ scale) prior to modeling to minimize correlation among terms. Terms not statistically significant (<90% confidence) were dropped from the model one at a time by the backward stepwise modeling technique. Graphs of these empirically derived models are shown in Figures 3, 4, 6, 8, 9, and 10.

RESULTS AND DISCUSSION

Preparation conditions and resulting properties of MTMS and BTMSPA aerogels, made in either acetonitrile or acetone are listed in Table 1 (polyurethane/urea reinforced aerogels) and Table 2 (nonreinforced aerogels). BTMSPA, a silane precursor containing a secondary amine, serves as a base catalyst for gelation as well as a reactive site for polymerization with the tri-isocyanate, Desmodur N3300A, shown in Scheme 1. The water/total silicon mole ratio, *r*, used in the initial hydrolysis and condensation of silane precursors is calculated based on the number of moles of water over the total moles of silicon (taking into account that BTMSPA

Scheme 2. Mechanism for Cross-Linking with Tri-Isocyanate, Including Chain Extension Reaction Due to Excess Water

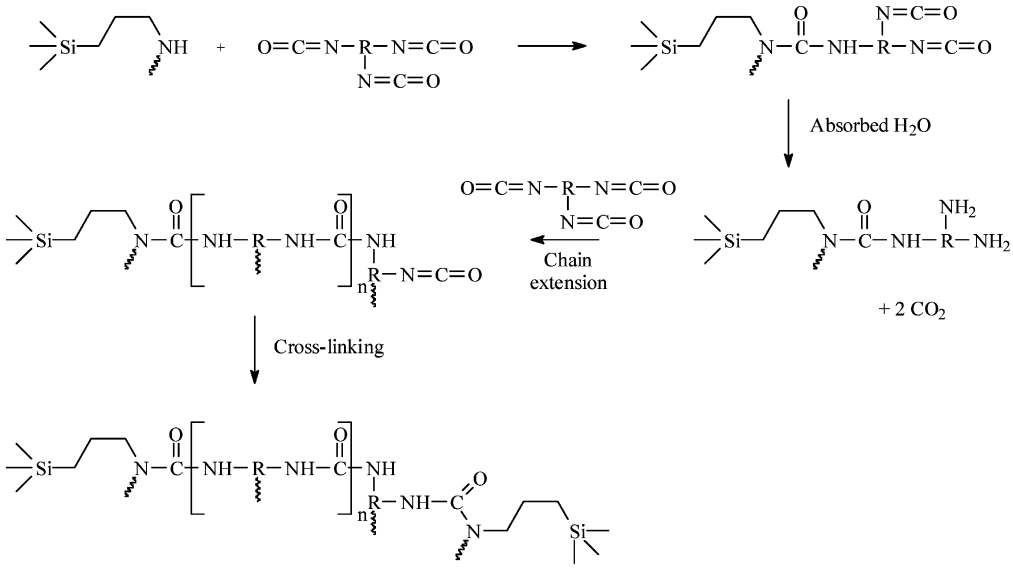

contributes two moles of silicon per mole). According to Brinker and Scherer (23), an r of two is considered stoichiometric for hydrolysis and condensation. However, an excess of water is usually needed for complete reaction. In this study, we varied r from 2 to 5. In addition, the number of washes in clean solvent after gelation and before reacting with polymer was varied from 1 to 3. Washing removes water and alcoholic byproduct of condensation. As previously described, when isocyanates are used as the polymer reinforcement, the amount of water left in the gels after condensation also can affect the number of repeat units in the polymer cross-links (3). As shown in Scheme 2, excess water reacts with the isocyanate to generate an amine which can react with other isocyanates to extend the polymer chain before reacting with amines attached to the silicon surface. Too little water can result in incomplete hydrolysis of the starting silanes, whereas too much water can lead to too much polymer being incorporated into the aerogels. Hence, a balance between the amount of water needed for gelation and the amount of water remaining in the gels for chain extension is desirable.

Solid ^{29}Si and ^{13}C NMRs. Solid ^{29}Si NMR spectra of selected reinforced aerogel samples, prepared in acetonitrile, are shown in Figure 1 along with samples prepared from BTMSPA and MTMS alone. It is evident from comparing Figure 1d (MTMS derived sample) and Figure 1c (BTMSPA derived sample) that the Si peaks completely overlap at −66 ppm (T_3 peak) and −58 ppm (T_2 peak). Spectra of polymer reinforced aerogels produced from 1.65 M total silicon with 40 mol % coming from BTMSPA are shown in Figure 1a (using $r = 5$) and Figure 1b (using $r = 2$). The r value has very little effect on the gel formation as there is very little difference in the two spectra. Both have a large T_3 peak and a smaller T_2 side peak, indicating that extent of condensation is about the same at different r for samples made using 3 washes. The same is true when comparing samples made using one wash.

Solid ^{13}C NMR spectra of selected reinforced aerogel samples from the study are shown in Figure 2. The spectra all contain one peak at −3.7 ppm assigned to the methyl group from MTMS, and three methylene peaks at 10.9, 23.2, and 49.9 ppm from BTMSPA. Additional peaks in the spectra come from the methylenes (28 and 41.8 ppm) and carbonyls (148.3 and 157.7 ppm) of the tri-isocyanate cross-linker. Integration of the BTMSPA methylenes (peak A at 10.9 ppm) closest to the Si with the tri-isocyanate methylenes (peak B at 41.8 ppm) closest to the nitrogen can give an indication of the degree of polymer cross-linking (n value from Scheme 2) depending on preparation conditions. In the absence of chain extension reactions, the cross-linked structure would be as shown in Scheme 1, where one molecule of tri-isocyanate has reacted with three different amines on the gel backbone. This would give a ratio of peak B to peak A of 1. A ratio of less than 1 would indicate that some of the amine has not reacted. A ratio of more than 1 would indicate some degree of chain extension. The highest ratio of isocyanate to amine measured for aerogels prepared in acetonitrile, was 1.2 as shown in Figure 2a for a spectrum of the monolith from sample 7 made using the highest level of total silicon (1.65 mol/L), 80 mol % BTMSPA, an $r = 5$ and only one wash. The corresponding aerogel made in acetone (sample 32), shown in Figure 2b, shows more incorporation of isocyanate with a ratio of 1.6. As the total silicon concentration and mol % of BTMSPA are decreased to 0.75 mol/L, isocyanate to amine ratio decreases as shown in spectra in Figure 2c for acetonitrile derived monolith (sample 21) and 2d for acetone derived monolith (sample 37). In fact, for sample 21, no tri-isocyanate is incorporated, whereas 37 has a peak B:A ratio of 0.26, indicating that only a fourth of the amines are reacted.

Use of acetone as a solvent instead of acetonitrile increases the reaction with amine with isocyanate across the whole study, as shown in the empirical model for the extent of cross-linking based on the ratio of peak B:A integration

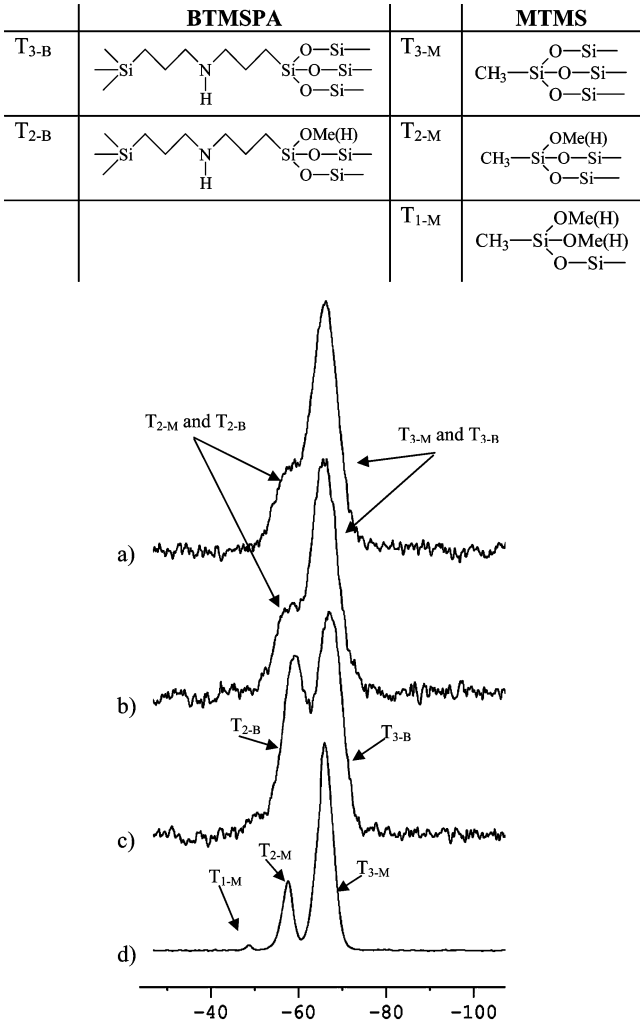

FIGURE 1. Solid ^{29}Si NMR spectra of samples from formulations listed in Table 1 as (a) 23 with $r = 5$ and (b) 28 with $r = 2$, and aerogels formulated from (c) BTMSPA alone and (d) MTMS alone. All samples shown were prepared in acetonitrile.

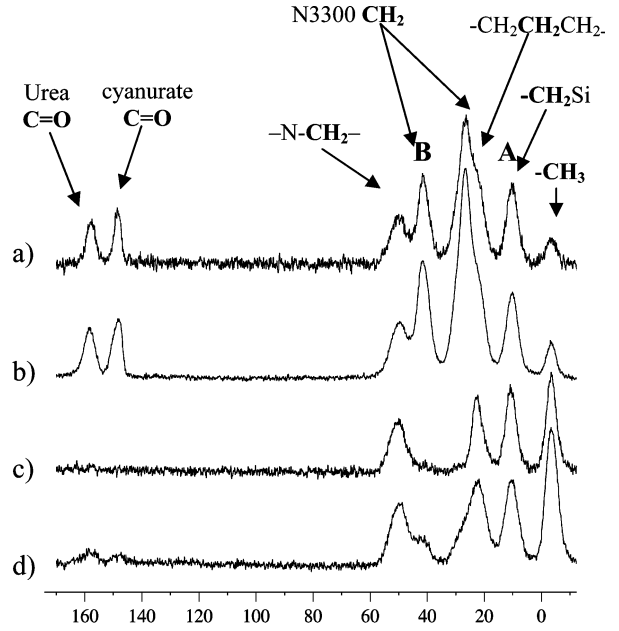

FIGURE 2. Solid ^{13}C NMR spectra of samples from formulations listed in Table 1. Sample spectra of aerogels made in (a) acetonitrile and (b) acetone were fabricated using 1.65 mol/L total Si with 80 mol % BTMSPA derived Si, whereas those in (c) acetonitrile and (d) acetone were fabricated from 0.75 mol/L total Si with 40 mol % BTMSPA derived Si. Peaks labeled as A (methylene from tri-isocyanate) and B (methylene from BTMSPA) were integrated to give tri-isocyanate to amine ratio modeled in Figure 3.

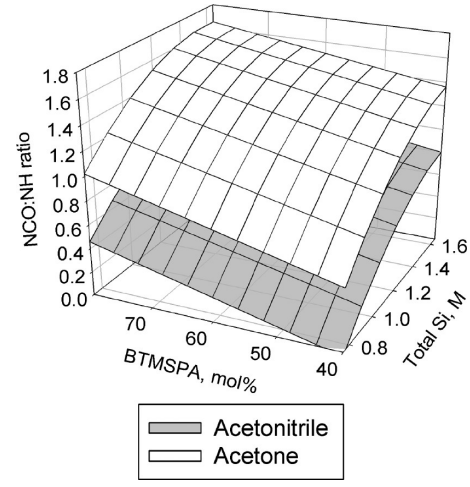

FIGURE 3. Empirical model of tri-isocyanate to amine ratio (integration of peak B to peak A, Figure 2) measured from integration of ^{13}C NMR spectra graphed vs BTMSPA fraction and total Si.

(standard error = 0.11, R^2 = 0.90) shown in Figure 3. Increasing total Si and fraction of BTMSPA derived Si also significantly increases the amount of cross-linking. An isocyanate:amine ratio of at least 1 (balanced stoichiometry as shown in Scheme 1) is produced in acetonitrile when 1.65 mol/L total Si and BTMSPA-derived Si of at least 60 mol % are used or with 80 mol % BTMSPA-derived Si and at least 1.2 mol/L total Si. For acetone-derived monoliths under these same conditions, chain extension, as shown in Scheme 2, becomes a factor.

A clue to why there is very little incorporation of tri-isocyanate at lower total Si and low BTMSPA fraction, especially in acetonitrile processed aerogels, comes from examining the BET surface area measured for the aerogel monoliths. The empirical model for BET surface area is shown in Figure 4a for nonreinforced aerogels (standard error = 48.9%, R^2 = 0.89). From the graph, it is clear that surface area decreases with decreasing total Si and decreasing BTMSPA fraction, especially in acetonitrile. As BTMSPA fraction is decreased, MTMS fraction increases, leading to more nonpolar methyl groups present on the silica surface. Interaction of the methyl groups with the more polar acetonitrile causes a collapse of the skeletal backbone of the gel. Acetone-prepared nonreinforced aerogels also decrease in surface area with decreasing total Si and BTMSPA fraction, but the effect is much smaller, most likely because acetone is less polar. Lower surface areas in the gels before cross-linking would mean less surface amine is available for reaction with isocyanate. The empirical model of BET surface area for those monoliths treated with cross-linker (standard error = 15.8%, R^2 = 0.97) is shown in Figure 4b. In addition to the reduction in surface area due to decreasing total Si and BTMSPA fraction seen in the nonreinforced aerogels, the surface area also decreases with increasing amount of polymer reinforcement. This is as would be

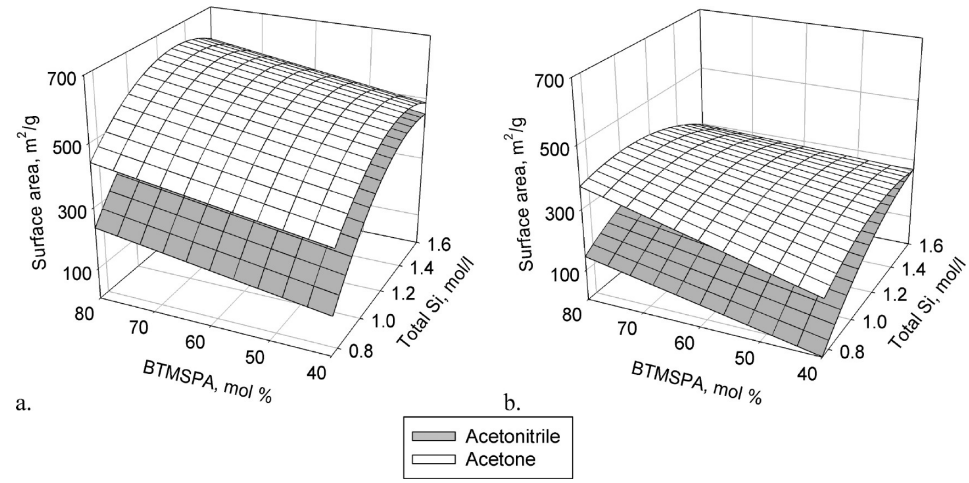

FIGURE 4. Empirical models of BET surface areas graphed vs total Si and BTMSPA fraction for (a) nonreinforced aerogels and (b) aerogels reinforced with tri-isocyanate.

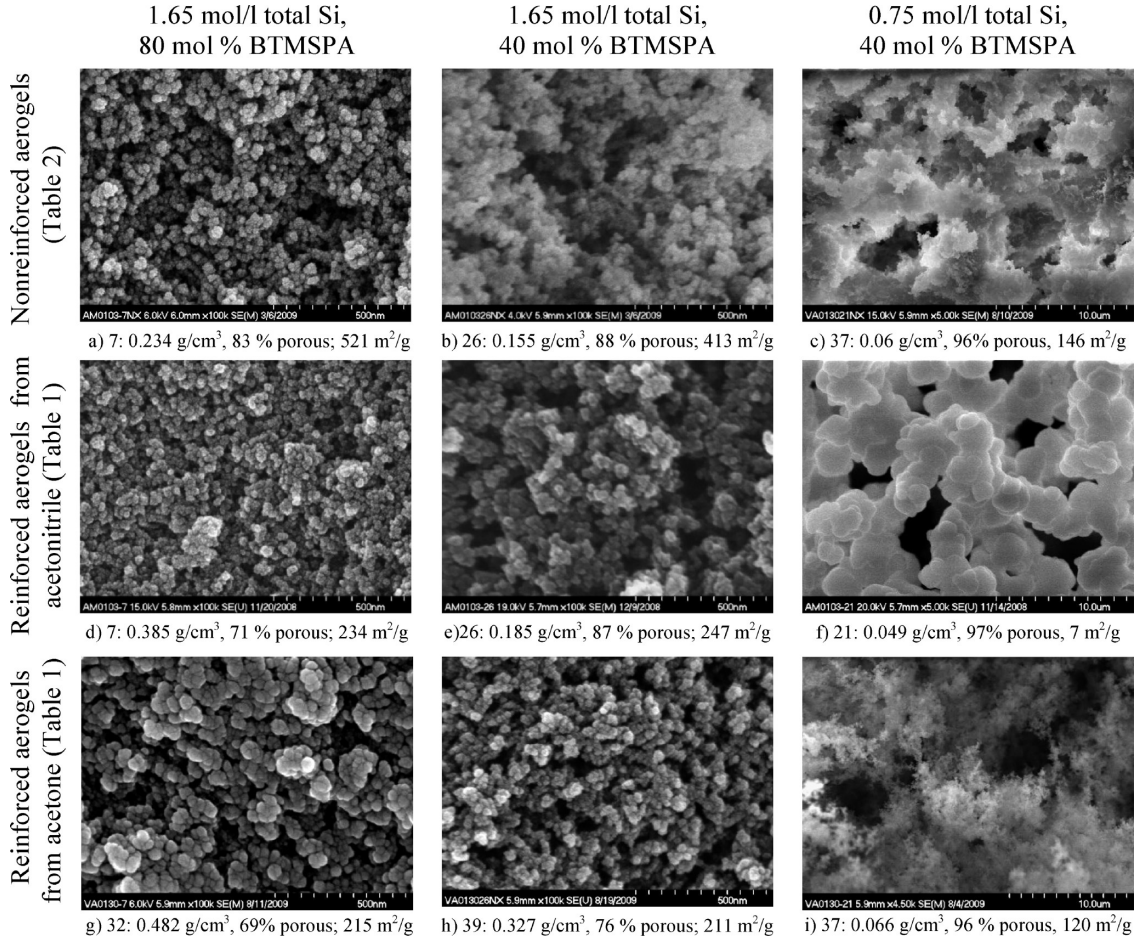

FIGURE 5. SEM images of select nonreinforced samples (a–c) from Table 2, compared to corresponding reinforced aerogels from Table 1 prepared using acetonitrile as solvent (d–f), and using acetone as solvent (g–i).

expected because of an increase in the amount of solid in the aerogels compared to nonreinforced aerogels. Also, small pores interior to the secondary particles may be blocked from nitrogen sorption because of polymer cross-linking, which would also reduce BET surface area.

Scanning electron micrographs (SEM) of select samples from the study shown in Figure 5 illustrate the differing morphologies arising from different processing conditions. Nonreinforced aerogels shown in Figure 5a–c illustrate the increase in particle size and decrease in surface area as total Si and BTMSPA fraction is reduced (noting that sample 37 from Table 2 shown in Figure 5c is at a different scale). For aerogels prepared in acetonitrile using 1.65 mol/L total Si, polymer cross-linking does not change the appearance of the gel structure as seen by comparing SEMs shown in images a and b in Figure 5 to those shown in images d and e in

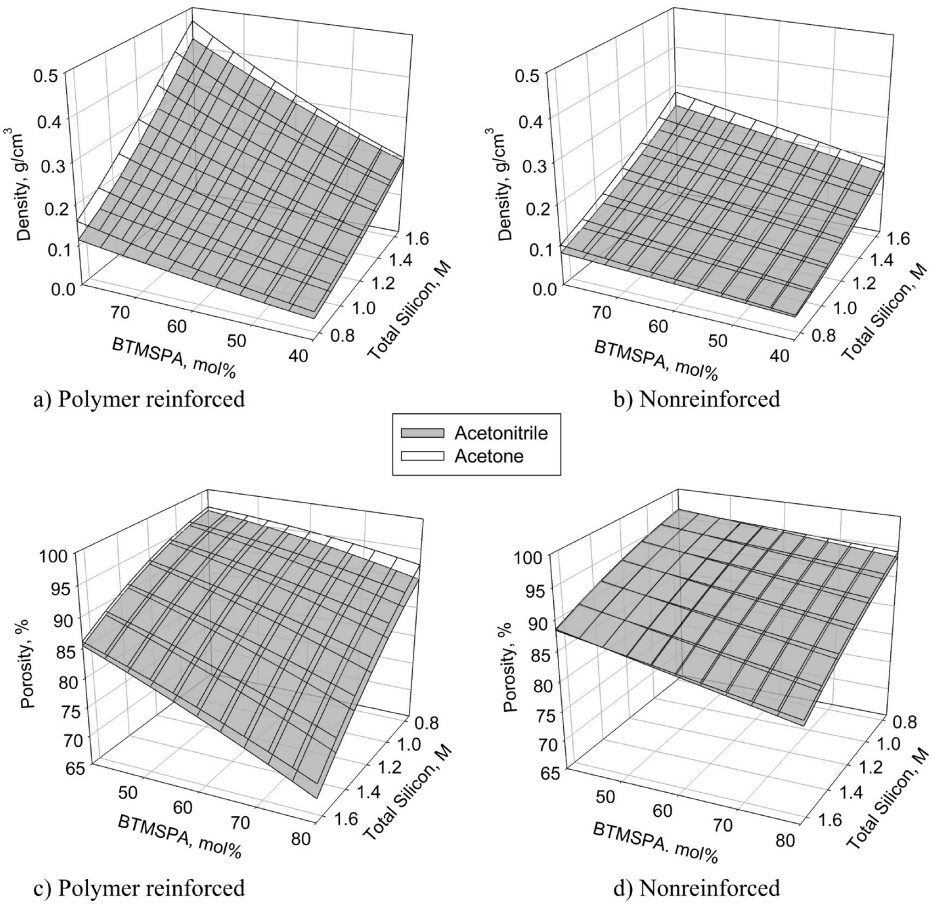

FIGURE 6. Empirical models graphed vs mol % of BTMPSA and total Si concentration of density (a, b) and porosity (c, d), comparing nonreinforced samples and polymer reinforced samples prepared using acetone or acetonitrile.

Figures 5, respectively, although the surface area is about halved in the reinforced samples. In contrast, particle sizes appear to be larger for the comparable polymer reinforced aerogel made in acetone using the highest total Si and highest BTMSPA (Figure 5g). This sample has the most amine content and the highest surface area before cross-linking. Hence, all of the amines are readily available for reaction with tri-isocyanate. For the polymer reinforced aerogel made in acetone using 1.65 mol/L total Si and 40 mol % BTMSPA (Figure 5h), the particle sizes again appear comparable to the acetonitrile-prepared sample shown in Figure 5e, although the density is much higher and the amount of isocyanate reacted per amine is about doubled over the acetonitrile prepared sample. It should also be noted that the monolith shown in Figure 5g has more polymer incorporated than that shown in Figure 5h. Though the sample shown in Figure 5h (run 39 from Table 1) has a larger ratio of isocyanate to amine (peak B:A), there is twice the amount of amine in the sample shown in Figure 5g (run 32 from Table 1). Reinforced aerogels prepared in acetone using 0.75 mol/L total Si (Figure 5i) are also similar in appearance to the comparable nonreinforced aerogels (Figure 5c). In fact, these samples are not that different in density, porosity or surface area, because there is very little polymer incorporated in the cross-linked sample (only about 20% of the amines are reacted.) The comparable acetonitrile prepared sample, shown in Figure 5f, in contrast, has very large particle sizes which are smoother in appearance, again demonstrating that the fine pore structure of the aerogel is lost under these conditions. Indeed, as previously discussed and evidenced by NMR, in this sample, almost no tri-isocyanate is incorporated.

Density, Porosity, and Dimensional Change. The empirical models derived for density of the polymer reinforced monoliths (standard error = 0.11, $R^2 = 0.90$) in Figure 6a, is compared to that of the nonreinforced aerogels (standard error = 0.35, $R^2 = 0.99$) in Figure 6b. For both nonreinforced and polymer reinforced aerogels, increasing total Si concentration and mol fraction of BTMSPA increases density both by adding more silica to the structure and more organic linking groups to the backbone. Increasing BTMSPA fraction increases density more for reinforced aerogels, especially at higher total Si because of an increase in amine sites available for tri-isocyanate reaction. However, because there is little polymer incorporated in formulations with the lowest total silicon and BTMSPA mol fraction as seen by NMR, similar densities are obtained for nonreinforced and reinforced samples under those conditions. Increasing Si to water ratio and decreasing the number of washes (not shown in the plots) also causes a small though significant increase in density.

The empirical models for porosity for reinforced aerogels (standard error = 0.72%, $r^2 = 0.99$) and nonreinforced

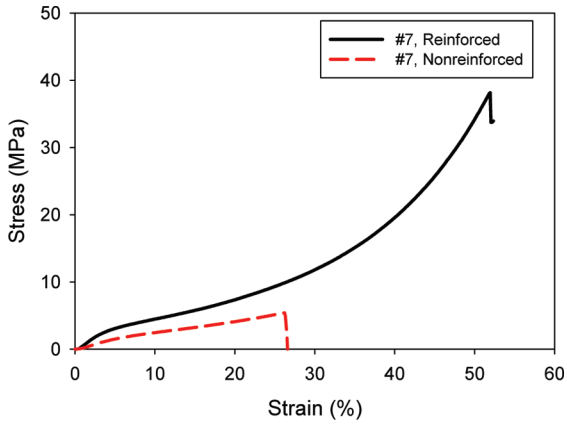

FIGURE 7. Typical stress–strain curves of a polymer reinforced aerogel (solid black line, $\rho = 0.385$ g/cm^3) compared to a nonreinforced aerogel (red dashed line, $\rho = 0.234$ g/cm^3), both prepared in acetonitrile.

aerogels (standard error = 0.55%, $r^2 = 0.99$), are shown in panels c and d in Figure 6, respectively. As is typically the case, porosity follows the opposite trends as density (noting that the x and y planes are rotated compared to panels a and b in Figure 6). Thus, increasing total Si concentration decreases porosity for both reinforced and nonreinforced aerogels. Increasing BTMSPA mol fraction tends to decrease porosity, though this effect is larger for the polymer reinforced aerogels. This is because increasing available amine sites from BTMSPA increases the amount of tri-isocyanate incorporation.

Of course, the density and porosity are also influenced by the dimensional change or shrinkage (%) of a monolith over the course of processing the aerogels. In this study, shrinkages were small, ranging from 0.4 to 12% for the polymer reinforced aerogels and 0.6 to 14% for the nonreinforced aerogels. BTMSPA fraction has the largest effect on shrinkage, which increases by up to 9% over the whole range for nonreinforced aerogels and up to about 6% for reinforced aerogels. The polymer reinforced aerogels tended to shrink 2–3% less than the nonreinforced aerogels especially at higher total Si concentration. The aerogels prepared in acetonitrile tended to shrink 1–2% less than those made in acetone. Overall, increasing total Si concentration has a minor impact on shrinkage for both nonreinforced and reinforced aerogels (~2% over the whole range).

Mechanical Properties. As an example, stress–strain curves from compression tests for reinforced and nonreinforced aerogels from formulation 7 from Tables 1 and 2 made using 1.65 total Si (80 mol % Si from BTMSPA) are shown in Figure 7. Elastic modulus from each compression test is calculated from the initial slope of the stress strain curves. As seen in the example curves, typically the modulus is slightly higher for the polymer reinforced samples while stress at break is much increased. Shown in Figure 8 are the empirical models for modulus graphed vs total Si concentration and mol fraction of BTMSPA for both nonreinforced aerogels (standard error = 0.19, $r^2 = 0.99+$) and polymer reinforced aerogels (standard error = 0.09, $r^2 = 0.99+$) made in acetone (Figure 8a) and acetonitrile (Figure 8b). Modulus increases with an increase in total silicon concentration and mol % of BTMSPA for both nonreinforced and reinforced aerogels. This is expected because, in a broad sense, modulus typically scales with density in aerogels. Aerogels prepared in acetone solvent also had higher modulus than those made in acetonitrile, because acetone-prepared aerogels contain more polymer and shrink slightly more than those prepared in acetonitrile. Note also that nonreinforced aerogels prepared in acetone had slightly higher modulus than those prepared in acetonitrile, possibly also due to slightly greater shrinkage contributing to an increase in density. Water ratio (not shown) also has a slight effect on modulus, increasing with an increasing amount of water for both acetone- and acetonitrile-prepared aerogels. As previously noted, increasing amount of water affects both the underlying silica gel structure (more complete hydrolysis) as well as the polymer cross-linking (chain extension). No significant effect on the number of washes before cross-linking was seen over and above random error.

Empirical models for maximum strength at break are shown in Figure 9 for nonreinforced aerogels (standard error = 0.58, $r^2 = 0.94$) and polymer reinforced aerogels (standard error = 0.35, $r^2 = 0.99$), using acetone as solvent (Figure 9a) and acetonitrile as solvent (Figure 9b) (24). As with modulus, in general, as the total Si concentration and BTMSPA mol fraction increases, the maximum stress increases. In addition, polymer reinforced aerogels are as much as an order of magnitude higher in maximum strength at break than their nonreinforced counterparts, indicating that the cross-linker indeed enhances the mechanical properties. Unlike modulus, no significant effect of water ratio was seen on the maximum stress, over and above random error. This suggests strength at break is not as sensitive to the degree of chain extension or condensation of silica gel structure. Because failure occurs during densification, it is the amount of material present that governs this property. The maximum strength at break for monoliths prepared in acetone at lower BTMSPA fraction is higher compared to those prepared in acetonitrile, because of the larger amount of polymer incorporated in the acetone aerogels.

An alternative approach to characterizing the overall strength in these aerogels is to examine toughness. The toughness of a material is the amount of energy required to deform a volume of material to its breaking point, and hence its units are J/m^3. Toughness analysis was performed as it was noted that polymer reinforced aerogels displayed not only higher stress at break than their native counterparts, but about 20% more strain at break on average. Toughness is calculated by taking the area under the stress–strain curve. Integration of the trend-line equation matching the stress–strain data, and having an R-squared value greater than 0.99, was performed for each stress–strain measurement. As an example, in the curves shown in Figure 7, strain at break is nearly double for the polymer reinforced aerogels. Note that this analysis is typically performed for experiments in tension loading, and direct comparisons to other systems outside this study should be made with caution.

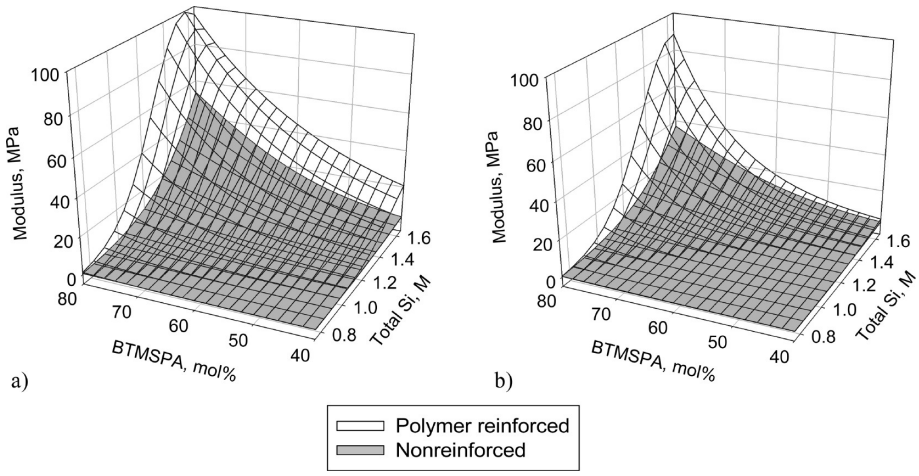

FIGURE 8. Empirical model of modulus graphed vs BTMSPA fraction and total Si of reinforced aerogels compared to nonreinforced aerogels made in (a) acetone and (b) acetonitrile.

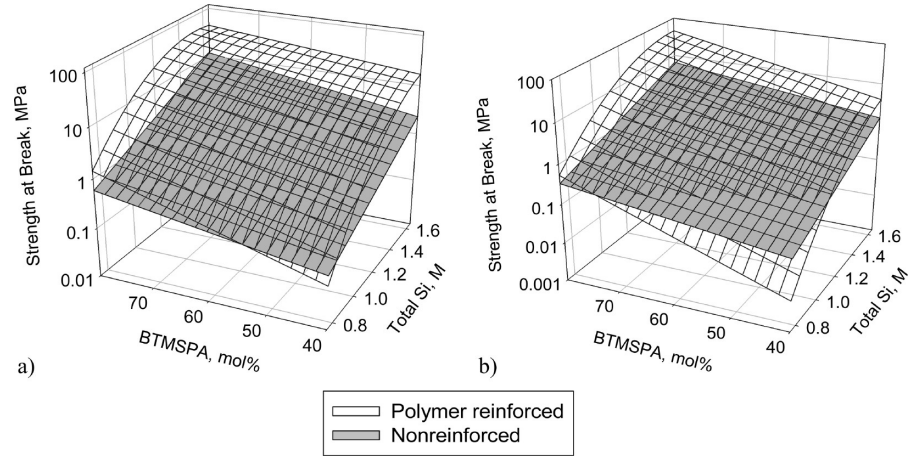

FIGURE 9. Empirical model of strength at break graphed vs BTMSPA fraction and total Si of reinforced aerogels compared to nonreinforced aerogels made in (a) acetone and (b) acetonitrile.

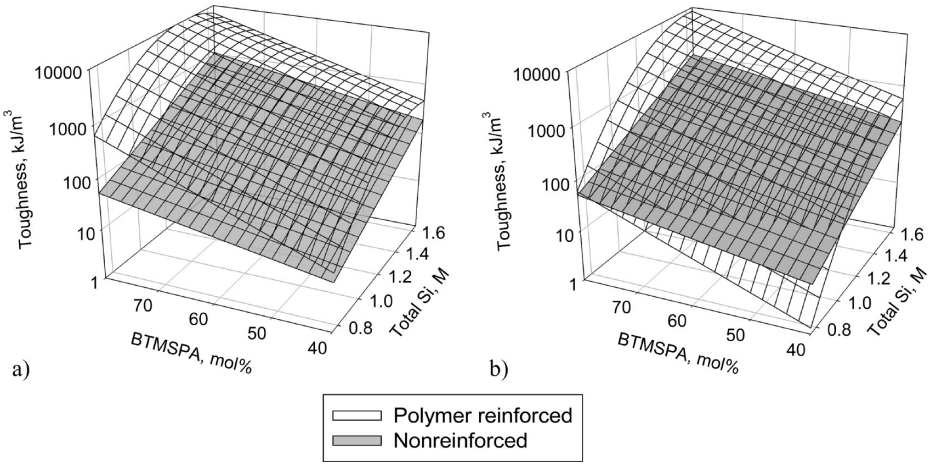

FIGURE 10. Empirical model of toughness graphed vs BTMSPA fraction and total Si of reinforced aerogels compared to nonreinforced aerogels made in (a) acetone and (b) acetonitrile.

Empirical models for toughness for nonreinforced (standard error = 0.69, r^2 = 0.92) and reinforced aerogels (standard error = 0.35, r^2 = 0.99) are shown in Figure 10 graphed vs total Si concentration and mol fraction BTMSPA for acetone prepared samples (Figure 10a) and for acetonitrile prepared samples (Figure 10b) (20). Polymer reinforced samples made using 80 mol % Si derived from BTMSPA show up to an order of magnitude increase in toughness over nonreinforced samples of the same composition. This improvement is of course attributable to the reinforcement effect of the polymer conformal coating. The overall trends for toughness are the same as those for strength at break, because of the shape of the compression curves. As the aerogels are compressed, they eventually undergo a densi-

fication as porosity is lost (25). When this occurs, a noticeable upturn in the stress–strain curve appears, as seen in the polymer reinforced sample in Figure 7. Ultimate failure normally occurs for the reinforced aerogels in this regime, and the values for stress of the aerogel under densification are significantly higher than that of the initial deformation. Hence, toughness follows the same trends as strength at break with as much as an order of magnitude increase over the nonreinforced aerogels. In addition, polymer reinforced aerogels prepared in acetone at low total Si concentration are higher in toughness than those prepared in acetonitrile, again because of the greater amount of polymer cross-linking in the acetone-derived aerogels. At high total Si concentration there is not as much difference in toughness between reinforced aerogels made in acetone or acetonitrile.

Graphs of the power law dependencies between the density, and compressive modulus, maximum stress at break and toughness for all formulations in the study (including acetonitrile and acetone runs) are shown in Figure 11. Power law relationships between modulus and density for silica aerogels (no organic groups) (26) are typically reported with an exponent of 3–3.7 depending on synthesis route and have been shown to depend most on the connectivity between particles (27). It has also been reported that the exponent for the power law dependency between the density and modulus for silica aerogels reinforced with isocyanates is higher (3.99 for base-catalyzed, reinforced aerogels), possibly because the lower-density, conformal coating of the polymer reinforces the structure more efficiently by increasing the neck regions between particles (2). As shown in Figure 11a, there is not much difference between the exponent b[1] for both reinforced and nonreinforced aerogels in this study (4.5 and 4.7, respectively), suggesting that the backbone in this case has more influence on modulus than the polymer cross-linking when organic linking groups are present. This is also similar to that reported for the power law relationship between modulus and density for polystyrene reinforced aerogels containing hexyl linking groups (b[1] = 5.1) (20). In that case, the hexyl links contribute similarly to the connectivity in the silica backbone as the dipropylamine linking groups do from BTSMPA in this study. Not surprisingly, maximum stress at break (Figure 11b) and toughness (Figure 11c) do show a greater influence on the power law dependence from polymer reinforcement. In both of these cases, the exponent b[1] increases from approximately 3 in the nonreinforced aerogels to greater than 4 for reinforced aerogels.

As previously noted (14, 15), flexibility and good recovery after compression are features of MTMS-derived aerogels. As a way of quantifying these properties for the aerogels from this study, the monoliths were taken through two consecutive compression cycles to 25% strain and allowed to recover for 30 min. The difference in the length of the samples before and after both tests is considered to be the amount of unrecovered strain and is listed in Tables 1 (polymer reinforced aerogels) and 2 (nonreinforced aerogels). The lower the unrecovered strain, the more elastic is

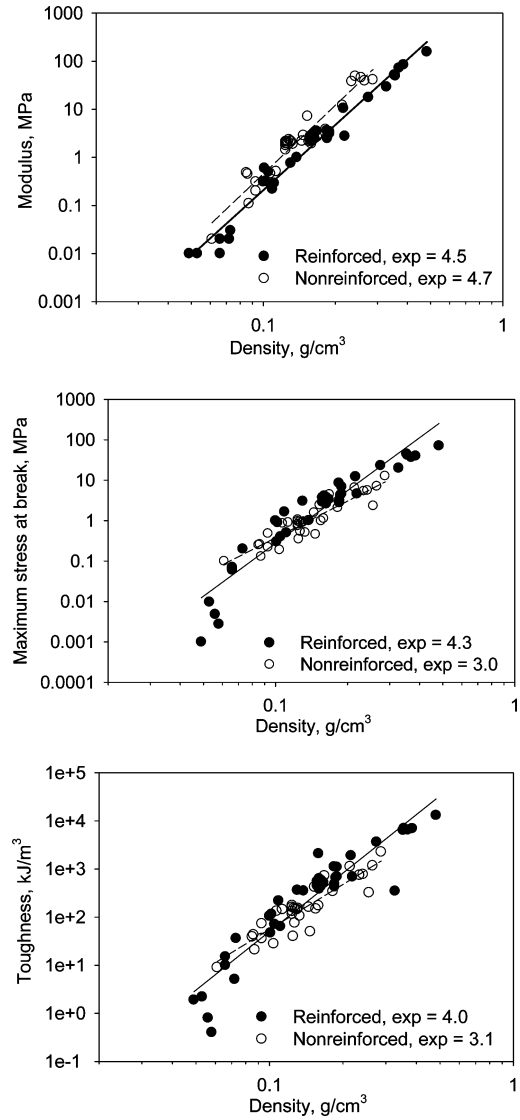

FIGURE 11. Power law dependency between the density and (a) compressive modulus; (b) maximum stress at break; and (c) toughness for all aerogel formulations.

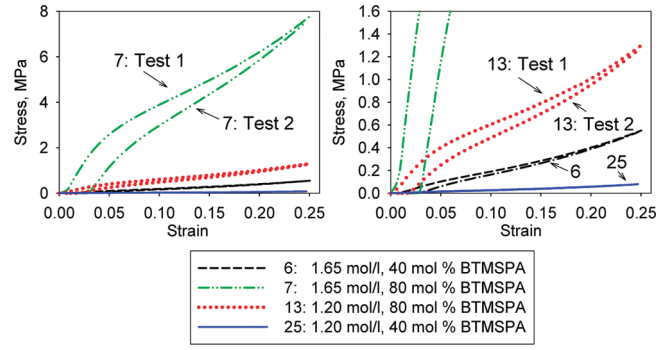

FIGURE 12. Typical stress–strain curves for a repeat compression tests on various polymer reinforced samples with different total silicon concentration and BTMSPA levels of monoliths prepared in acetonitrile.

the aerogel monolith. To illustrate, stress–strain curves for repeat compression tests to 25% strain of different polymer reinforced aerogels are compared in Figure 12. The pairs of lines in the graphs represent two subsequent stress–strain curves, labeled Test 1 and Test 2, from four different

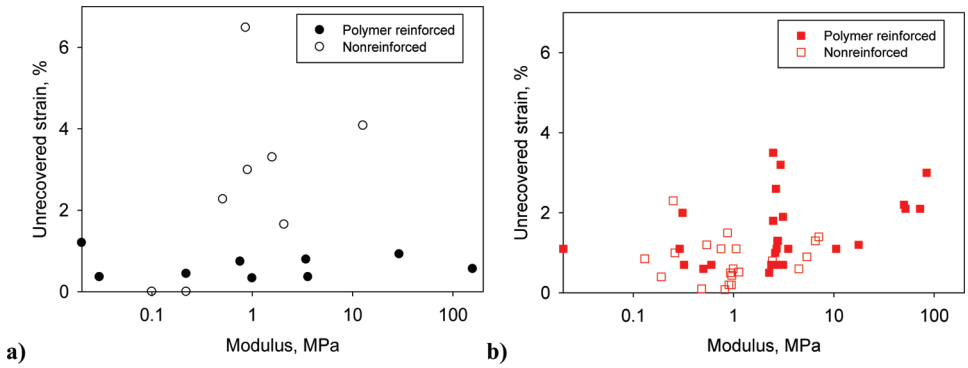

FIGURE 13. Graph of unrecovered strain vs modulus for all aerogels in study, showing polymer reinforced and nonreinforced aerogels made in (a) acetone and (b) acetonitrile.

formulations. For example, the curve labeled Test 1 in the graph on the left represents the first compression of sample 7 from Table 1 made from 1.6 mol/L total Si and 80 mol % Si from BTMSPA. The curve labeled Test 2 is the second compression. After both compressions and the recovery time, the sample length was reduced by 3% (i.e., there is about 3% unrecovered strain in the sample). In contrast, repeat compression cycles from formulation 13 (Table 1), labeled in the graph to the right, made using 1.2 mol/L total Si and 80 mol % BTMSPA derived Si shows about 1.1% unrecovered strain after both tests. Other pairs of curves in the graphs represent other formulations with lower modulus and similar recovery.

Note in Tables 1 and 2 that most of the nonreinforced and reinforced aerogels made using MTMS and BTMSPA exhibit low unrecovered strain (samples spring back from compression), consistent with good elasticity. Although typically there is a trade-off between modulus and recovery after compression, in this study the trade off is very small, with even the highest modulus reinforced aerogels exhibiting only up to 3.8% unrecovered strain for those made in acetonitrile and up to 1.2% for those made in acetonitrile. Figure 13 shows graphs of modulus vs unrecovered strain for acetone (Figure 13a) and acetonitrile (Figure 13b) derived aerogels. Although there is a slight increase in unrecovered strain as modulus increases for the nonreinforced aerogels and for the polymer reinforced aerogels made in acetonitrile, the polymer reinforced aerogels made in acetone show 0−1% unrecovered strain across the whole range of modulus. Because the acetone-derived samples also have higher incorporation of tri-isocyanate, this indicates that hexyl linkages from the tri-isocyanate contribute to the flexibility of the overall network.

CONCLUSIONS

The combination of MTMS and BTMSPA used in the silica backbone provides enhanced elastic properties to tri-isocyanate reinforced silica aerogels. The dipropylamine spacers from BTMSPA contribute flexible linking groups in the silica structure, as well as reactive sites via their secondary amines for reaction with a triisocyanate, Desmodur N3300A. The trifunctional isocyanate provides an extended degree of branching or cross-linking, resulting in up to an order of magnitude increase in compressive strength of the aerogel monoliths while the overall flexibility arising from the underlying silica structure is maintained. The compressive moduli of the reinforced aerogel monoliths in this study range from 0.001 to 84 MPa for those prepared in acetonitrile and 0.01 to 158 MPa for their counterparts made in acetone. All formulations across this entire range of modulus recover nearly all of their length after two compressions to 25% strain. This result represents an order of magnitude improvement in modulus for aerogels which recover completely after compression, compared to previous polymer reinforced aerogels studied. Higher total silicon concentration and mole fraction of Si derived from BTMSPA result in larger amounts of tri-isocyanate incorporation and enhanced compressive strength and toughness. In addition, the strongest monoliths still have surface areas greater than 200 m^2/g measured by BET and densities less than 0.5 g/cm^3, only a 50% increase in density over the nonreinforced aerogels of the same formulation. In contrast, at low total silicon concentration and low mol % of BTMSPA-derived Si, little or hardly any reaction occurred with tri-isocyanate, resulting in modest or no improvement in mechanical properties. These formulations also produced monoliths with lower surface area and larger pore sizes. In general, the use of acetone as a solvent in preparation of aerogels results in higher BET surface areas and better mechanical properties compared to those made in acetonitrile. These results may be enabling for aerospace applications such as EDL systems and EVA suits, which demand a combination of superior insulation durability and flexibility.

Acknowledgment. Financial support from NASA's Fundamental Aeronautics Program is gratefully acknowledged. The authors also thank Mr. Dan A. Scheiman for pycnometry measurements, Ms. Anna Palczer for the BET surface area data, and Bayer Corporation for supplying the Desmodur N3300A.

REFERENCES AND NOTES

(1) (a) Jones, S. M. *J. Sol−Gel Sci. Technol.* **2006**, *40*, 351–357. (b) Fesmire, F. E. *Cryogenics* **2006**, *46*, 111–117. (c) Pierre, A. C.; Pajonk, G. M. *Chem. Rev.* **2002**, *102*, 4243–4265.

(2) Zhang, G.; Dass, A.; Rawashdeh, A.-M. M.; Thomas, J.; Counsil, J. S.; Sotirious-Leventis, C.; Fabrizio, E. F.; Ilhan, F.; Vassilaras, P.; Scheiman, D. A.; McCorkle, L.; Palczer, A.; Johnston, J. C.; Meador, M. A. B.; Leventis, N. *J. Non-Cryst. Solids* **2004**, *350*, 152–164.

(3) Meador, M. A. B.; Capadona, L. A.; McCorkle, L.; Papadopoulos, D. S.; Leventis, N. *Chem. Mater.* **2007**, *19*, 2247.

(4) Capadona, L. A.; Meador, M. A. B.; Alumni, A.; Fabrizzio, E. F.; Vassilaras, P.; Leventis, N. *Polymer* **2006**, *47*, 5754.
(5) Meador, M. A. B.; Fabrizzio, E. F.; Ilhan, F.; Dass, A.; Zhang, G.; Vassilaras, P.; Johnston, J. C.; Leventis, N. *Chem. Mater.* **2005**, *17*, 1085.
(6) Boday, D. J.; Stover, R. J.; Muriithi, B.; Keller, M. W.; Wertz, J. T.; Obrey, K. A. D.; Loy, D. A. *ACS Appl. Mater. Interfaces* **2009**, *1* (7), 1364–1369.
(7) (a) Ilhan, U. F.; Fabrizzio, E. F.; McCorkle, L.; Scheiman, D. A.; Dass, A.; Palczer, A.; Meador, M. A. B.; Johnston, J. C.; Leventis, N. *Mater. Chem.* **2006**, *16*, 3046–3054. (b) Mulik, S.; Sotiriou-Leventis, C.; Churu, G.; Lu, H.; Leventis, N. *Chem. Mater.* **2008**, *20* (15), 5035–5046.
(8) Paul, H. L.; Diller, K. R. *J. Biomech. Eng.* **2003**, *125*, 639–647.
(9) Fesmire, J. E. *Cryogenics* **2006**, *46*, 111–117.
(10) Braun, R. D.; Manning, R. M. *J. Spacecr. Rockets* **2007**, *44*, 310–323.
(11) Brown, G. J.; Lingard, J. S.; Darley, G. D.; Underwood, J. C. *19th AIAA Aerodynamic Decelerator Systems Technology Conference and Seminar*; Williamsburg, VA, May 21−24, 2007; American Institute of Aeronautics and Astronautics: Reston, VA, 2007; p 2543.
(12) Reza, S.; Hund, R.; Kustas, F.; Willcockson, W.; Songer, J. *19th AIAA Aerodynamic Decelerator Systems Technology Conference and Seminar*; Williamsburg, VA, May 21−24, 2007; American Institute of Aeronautics and Astronautics: Reston, VA, 2007; p 2516.
(13) Kramer, S. J.; Rubio-Alonso, F.; Mackenzie, J. D. *Mater. Res. Soc. Symp. Proc.* **1996**, *435*, 295–299.
(14) Rao, A. V.; Bhagat, S. D.; Hirashima, H.; Pajonk, G. M. *J. Colloid Interface Sci.* **2006**, *300*, 279.
(15) (a) Kanamori, K.; Aizawa, M.; Nakanishi, K.; Hanada, T. *Adv. Mater.* **2007**, *19*, 1589–1593. (b) Kanamori, K.; Aizawa, M.; Nakanishi, K.; Hanada, T. *J. Sol−Gel Sci. Technol.* **2008**, 48.
(16) Finlay, K.; Gawryla, M. D.; Schiraldi, D. A. *Ind. Eng. Chem. Res.* **2008**, *47*, 615–619.
(17) Pushpadass, H. A.; Weber, R. W.; Hanna, M. A. *Ind. Eng. Chem. Res.* **2008**, *47*, 4736–4742.
(18) Park, K. W.; Him, G. H. *J. Appl. Polym. Sci.* **2009**, *112*, 1845–1849.
(19) Rezaeian, I.; Jafari, S. H.; Zahedi, P.; Ghaffari, M.i; Afradian, S. *Polym. Adv. Technol.* **2009**, *20*, 487–492.
(20) Nguyen, B. N.; Meador, M. A. B.; Tousley, M. E.; Shonkwiler, B.; McCorkle, L.; Scheiman, D. A.; Palczer, A. *ACS Appl. Mater. Interfaces* **2009**, *1* (3), 621–630.
(21) Meador, M. A. B.; Weber, A.; Hindi, A.; Naumenko, M.; McCorkle, L.; Quade, D.; Vivod, S. L.; Gould, G. L.; White, S.; Deshpande, K. *ACS Appl. Mater. Interfaces* **2009**, *1*, 894–906.
(22) Vivod, S. L.; Meador, M. A. B.; Nguyen, B. N.; Perry, R. *Polym. Prepr.* **2009**, *50* (1), 119.
(23) Brinker, C. J. Scherer, G. W. *Sol−Gel Science: The Physics and Chemistry of Sol−Gel Processing*; Academic Press: San Diego, 1990.
(24) It should be noted that nonreinforced aerogels made using the lowest total Si and low BTMSPA fraction are too fragile to be tested. As a result, secondary effects of total Si and BTMSPA concentration were not significant in the empirical models for toughness and strength at break which are based on only the available data points. Hence, where the graphs shown in Figures 9b and 10b seem to show that nonreinforced aerogels made with the lowest combination of total Si and BTMSPA fraction have better properties than the polymer reinforced aerogels, this is not the case.
(25) (a) Katti, A.; Shimpi, N.; Roy, S.; Lu, H.; Fabrizio, E. F.; Dass, A.; Capadona, L. A.; Leventis, N. *Chem. Mater.* **2006**, *18*, 285–296. (b) Leventis, N.; Sotiriou-Leventis, C.; Mulik, S.; Dass, A.; Schnobrich, J.; Hobbs, A.; Fabrizio, E. F.; Luo, H.; Churu, G.; Zhang, Y.; Lu, H. *J. Mater. Chem.* **2008**, *18*, 2475–2482. (c) Luo, H.; Churu, G.; Schnobrich, J.; Hobbs, A.; Fabrizio, E. F.; Dass, A.; Mulik, S.; Sotiriou-Leventis, C.; Lu, H.; Leventis, N. *J. Sol−Gel Sci. Technol.* **2008**, *48*, 113–134.
(26) For example, see Pekala, R. W.; Hrubesh, L. W.; Tillotson, T. M.; Alviso, C. T.; Poco, J. F.; LeMay, J. D. *Mater. Res. Soc. Symp. Proc.* **1991**, *207*, 197–200.
(27) Woigner, T; Reynes, J.; Hafidi, A. A.; Beurroies, I.; Phalippou, J. *J. Non-Cryst. Solids* **1998**, *241*, 45–52.

AM100081A